

Article

Characteristics and Catalytic Properties of Ni/Ti-Si Composite Oxide Catalysts via CO₂ Hydrogenation

Jakrapan Janlamool and Bunjerd Jongsomjit*

Center of Excellence on Catalysis and Catalytic Reaction Engineering,
Department of Chemical Engineering, Faculty of Engineering,
Chulalongkorn University, Bangkok 10330, Thailand
*E-mail: bunjerd.j@chula.ac.th

Abstract. In the present work, the effects of Ti addition on the characteristics and catalytic properties of the different silica-based supported nickel (Ni) catalysts were investigated. The different supports, such as the spherical silica particle (SSP), MCM41, TiSSP, and TiMCM were synthesized and used to prepare the Ni catalysts having 20 wt% of Ni loading for CO₂ hydrogenation under methanation. The different supports and catalysts were characterized by means of N₂ physisorption, XRD, SEM/EDX, XPS, TPR, and CO chemisorption. The TiO₂ was present in the anatase form after catalyst calcination. The addition of Ti can play important roles on the characteristics and catalytic properties of Ni catalysts by: (i) facilitating the reduction of Ni oxides species strongly interacted with support, (ii) preventing the formation of silicate compounds, and (iii) promoting the CO and CO₂ dissociation resulting in complete inhibition of the reverse water-gas shift (RWGS) reaction, especially at high temperature. Based on CO₂ hydrogenation, the NiTiMCM exhibited the highest activity and stability.

Keywords: CO₂ hydrogenation, titania-silica, nickel catalysts, methanation.

ENGINEERING JOURNAL Volume 21 Issue 7

Received 18 February 2017

Accepted 27 April 2017

Published 29 December 2017

Online at <http://www.engj.org/>

DOI:10.4186/ej.2017.21.7.45

1. Introduction

The nickel-based catalysts are widely applied in many heterogeneous catalytic reactions, such as hydrogenation of aromatic hydrocarbon [1], CO₂ reforming of CH₄ [2] oxidative dehydrogenation of ethane [3] and methanation of CO₂ [4, 5]. The hydrogenation of CO₂ is significantly used in the purification of ammonia feed stocks and methanation of coal-derived [6]. The highly-dispersed supported nickel has been extensively used as the catalysts in the catalytic hydrogenation of CO₂ to methane. The catalytic hydrogenation of carbon monoxide and carbon dioxide produces a large variety of products ranging from methane and methanol to higher molecular weight alkanes, alkenes and alcohols [7-9]. There are two major mechanisms proposed for the methanation of CO₂. First, one involves transformation of CO₂ to CO prior to methanation [8]. The other involves pathways, in which the transformation of CO₂ to CO are not required [10].

Transition metal oxides are one of the most important classes of oxides and mixed oxides extensively used in various catalysts. Mostly, supports such as, Al₂O₃, SiO₂, ZrO₂ and TiO₂ can efficiently affect on activity and selectivity properties of the active phase for CO₂ hydrogenation [11]. Previous research showed that the nickel catalysts supported on Al₂O₃ prepared by coprecipitation method exhibited high methanation activity and low CO production level in catalytic methanation of CO₂ [5]. Furthermore, the prepared rice husk ash and rice husk ash-alumina supported nickel catalyst also exhibited high selectivity in catalytic methanation of CO₂ hydrogenation [4]. Recently, the development of materials represents the TiO₂-SiO₂ composite as a novel class of metal oxide materials. It was attractively used as effective supports and catalysts for a wide variety of catalytic reactions. Mesoporous SiO₂, such as MCM41 and hexagonal mesoporous silica (HMS), possess sufficiently high surface area, thermal stability, excellent mechanical strength and uniform pore sizes [12]. The TiO₂ can modify the metal-support interaction and hydrogenation activity [1]. It can be added only in a small amount with other oxides to improve surface characteristics, thermal stability and surface acidity of the composite catalysts [1, 8]. The TiO₂-SiO₂ composite is generally synthesized by flame hydrolysis, impregnation, coprecipitation and sol-gel methods [1] by adding titanium precursor into the silica framework. The ordinary method effectively used for preparation of TiO₂-SiO₂ composite was sol-gel method. The titanium distribution in the TiO₂-SiO₂ composite depends on the method of preparation [1]. The effective method used is sol-gel hydrolysis because in which a capability to control the textural and surface properties of the mixed oxides, resulting in the novel properties occurrence [1, 8]. Recently, we reported that Ti can play the important roles in the properties of cobalt supported on Ti-Si composite oxide material such as preventing the silicate compounds and facilitating the reduction of Co oxides species, which are strongly interacted with support [8]. Although activity via CO₂ hydrogenation can be improved with the presence of Ti in the silica-based supported cobalt catalyst, the reverse water-gas shift (RWGS) reaction still occurred even at low reaction temperature (220°C) [8]. Thus, alternative metal such as nickel could be more promising.

The present research focuses on the fabrication of the Ti-Si composite oxides used as support for nickel catalysts. First, the mesoporous silica, such as spherical silica particle (SSP) and MCM41 were prepared by the sol-gel method. Then, titanium isopropoxide was introduced into the silica framework by hydrolysis to obtain the Ti-Si composite oxide. The nickel catalysts were prepared by direct impregnation of nickel precursor onto silica and Ti-Si composite oxide framework. The characteristics and catalytic behaviors via CO₂ hydrogenation under methanation condition were investigated and further discussed in more detail.

2. Experimental

2.1. Materials

Chemicals as follows were used ; titanium isopropoxide 97% TiPOT (Aldrich), tetraethyl orthosilicate 98% TEOS (Aldrich), ammonia 30% (Panreac), ethanol 99.99% (J.T. Baker), cetyltrimethylammonium bromide CTAB (Aldrich), isopropanol (QREc), nickel (II) nitrate hexahydrate 98% Ni(NO₃)₂·6H₂O (Aldrich).

2.2. Support and Nickel Catalyst Preparation

The silica supports were synthesized by using a sol-gel reaction. The composition of the synthesis gel had following molar ratio: 1 TEOS : 0.3 CTAB : 11NH₃ : e Ethanol : 144 H₂O. Molar ratios of ethanol addition (e) were varied at 0 and 58 for the preparation of MCM41 and SSP, respectively [8]. The mixed solution was

further stirred for 2 h at room temperature. The white precipitate was then collected by filtration and washed with deionized water. The dried sample was calcined at 550°C for 6 h with a heating rate of 10°C/min in air.

The desired amount of titanium isopropoxide (ca. 25 wt% of TiO₂) was dissolved in isopropanol (using 1:3 w/w of support : isopropanol). The silica sample was added into the solution and stirred for 1 h. Hydrolysis was performed by addition of ammonia (H₂O : TiPOT = 4:1). The sol was further stirred for 20 h at room temperature. Then, the sample was dried at 110°C for 24 h. Finally, the samples were calcined at 850°C for 2 h in a muffle furnace.

The nickel catalysts having 20 wt% of Ni were prepared by the incipient wetness impregnation using aqueous solution of nickel (II) nitrate hexahydrate [Ni(NO₃)₂·6H₂O]. The catalysts were dried at 110°C for 12 h, and then calcined in air at 500°C for 4 h.

Nomenclature of sample is given as follows; SSP and MCM refer to spherical silica and MCM-41, respectively. Furthermore, TiSSP and TiMCM refer to titania-spherical silica composite and titania-MCM-41 composite, respectively. For catalysts samples, NiX refers to nickel catalyst supported on the X support as mentioned above.

2.3. Catalyst Characterization and Reaction Test

The various supports and nickel catalysts were characterized by several techniques as follows:

N₂ physisorption: N₂ physisorption (N₂ adsorption at -196°C in a Micromeritics ASPS 2020) was performed to determine surface areas of the various supports and nickel catalysts.

X-ray diffraction (XRD): XRD was used to determine the phase composition of the different supports and catalysts using SIEMENS D 5000 X-ray diffractometer with CuK_α radiation with Ni filter in the 2θ range of 20-80 degrees with resolution of 0.04°.

Temperature programmed reduction (TPR): TPR was used to determine the reducibility and reduction temperature of the nickel catalysts. Approximately, 0.05 g of catalyst sample was used in the operation and temperature ramping from 35°C to 800°C at 10°C/min. The carrier gas was 10 % H₂ in Ar. A thermal conductivity detector (TCD) was used to measure the amount of hydrogen consumption. The calibration of hydrogen consumption was performed with bulk nickel oxide (NiO) at the same condition.

CO chemisorption: The static CO chemisorption at room temperature on the reduced catalysts was used to determine the number of reduced surface nickel metal atoms. CO chemisorption was carried out following the procedure using a Micromeritics Pulse Chemisorb 2750 instrument. Prior to chemisorption, the catalysts were reduced at 350°C for 3 h after ramping up at a rate of 10°C/min. After that, 30 μl of carbon monoxide was injected into catalyst and repeated until the desorption peaks were constant at room temperature. Amounts of carbon monoxide adsorption on catalyst are proportional to the number of active sites.

Scanning electron microscopy (SEM) and dispersive X-ray spectroscopy (EDX): SEM (JEOL mode JSM-5800LV) and EDX (Link Isis Series 300) were used to determine the morphology and elemental distribution of the catalyst particles. The crystallite size and nickel distribution of catalyst samples were observed using JEOL-JEM 200CX transmission electron microscope operated at 100 kV.

X-ray photoelectron spectroscopy (XPS): The XPS analysis was performed originally using an AMICUS spectrometer equipped with a Mg K_α X-ray radiation. For a typical analysis, the source was operated at voltage of 15 kV and current of 12 mA. The pressure in the analysis chamber was less than 10⁻⁵Pa.

Reaction study: CO₂ hydrogenation was performed to determine the overall activity and selectivity of the catalysts. Typically, 0.1 g of catalyst was packed in a fixed-bed microreactor. The catalyst sample was reduced *in situ* in flowing H₂ (50ml/min) at 350°C for 3 h. After reduction, a flow rate of Ar = 8 ml/min and 8.8% CO₂ in H₂ = 22 ml/min was fed into the reactor. The CO₂ hydrogenation was carried out at 220, 270 and 320°C in atmospheric pressure. The effluents were taken in 1 h interval and analyzed by gas chromatography. The steady state was reached within 6 h.

3. Results and Discussion

The morphology of spherical silica particle (SSP) and MCM-41 was characterized by scanning electron microscopy (SEM). The different morphology of between both silica samples was due to the SSP prepared using the large amount of ethanol, while MCM-41 was synthesized without alcohol. Figure 1 (left) shows the SEM images of SSP that reveals small, regular and spherical shape having size ranging from 0.2 to 0.8 μm

with an average size of ca. 0.6 μm . The MCM-41 support displays morphology of regular type with rod shape as seen in Fig. 1 (right).

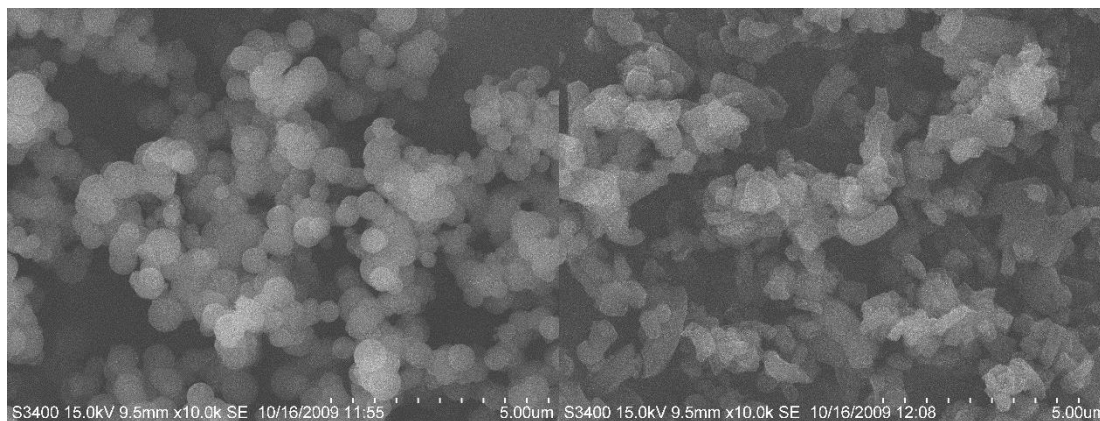


Fig. 1. The SEM images of the spherical silica particle (left) and MCM-41 (right).

The physical properties of the samples were obtained from the XRD and N_2 physisorption data. The XRD patterns and BET surface area for all support samples are shown in Fig. 2 (left) and Table 1, respectively.

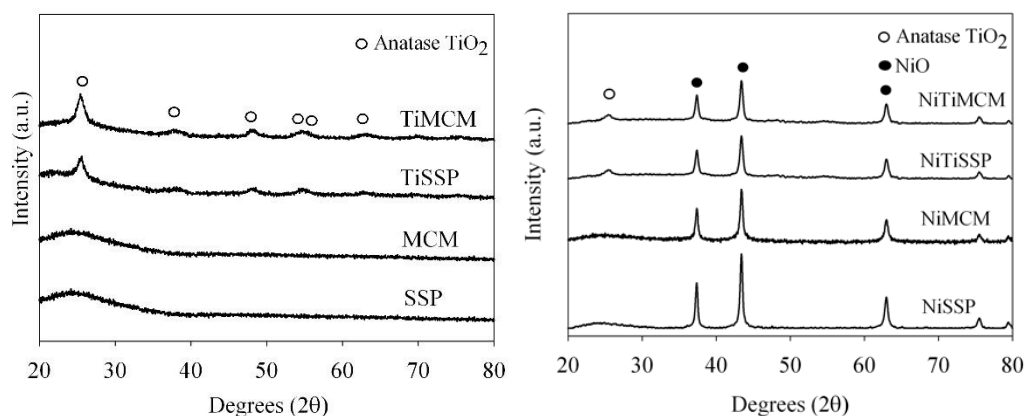


Fig. 2. XRD patterns of different supports (left) and different nickel catalysts (right).

The SSP and MCM supports exhibited the XRD patterns of amorphous silica indicating only a broad peak observation at 20-30°. After the TiO_2 was introduced into the mesoporous SiO_2 surface (SSP and MCM) via hydrolysis of titanium isopropoxide and calcined at 850°C, both TiSSP and TiMCM were obtained. The composite supports also exhibited the XRD patterns for titania being present in the anatase form (2θ of 25, 37, 48, 54, 56 and 75°) [8, 9]. Figure 2 (right) shows the XRD patterns of the calcined Ni catalysts. The attractive XRD peaks of NiO also display the strong intensity at 37.3, 43.3, 62.8 and 75.5° [1] for all Ni catalysts. Moreover, NiO peak resulted in the less appearance of the XRD peak of anatase titania crystalline at 25.3° for NiTiSSP and NiTiMCM. The surface areas of the silica samples were remarkably high as expected. However, after the TiO_2 was introduced into the mesoporous SiO_2 surface, the BET surface area of TiSSP and TiMCM were remarkably low ca. 385 and 137 m^2/g , respectively. It was due to the addition of titania into the silica framework resulting in particle sintering and the particle agglomeration. In addition, the BET surface areas for all nickel catalysts for different supports were much less than their corresponding supports as seen in Table 1. In addition, the nitrogen adsorption-desorption isotherm of supports and nickel catalysts are shown in Fig. 3. All of the isotherm are type IV having H1 hysteresis with a featured capillary condensation in the mesoporous material.

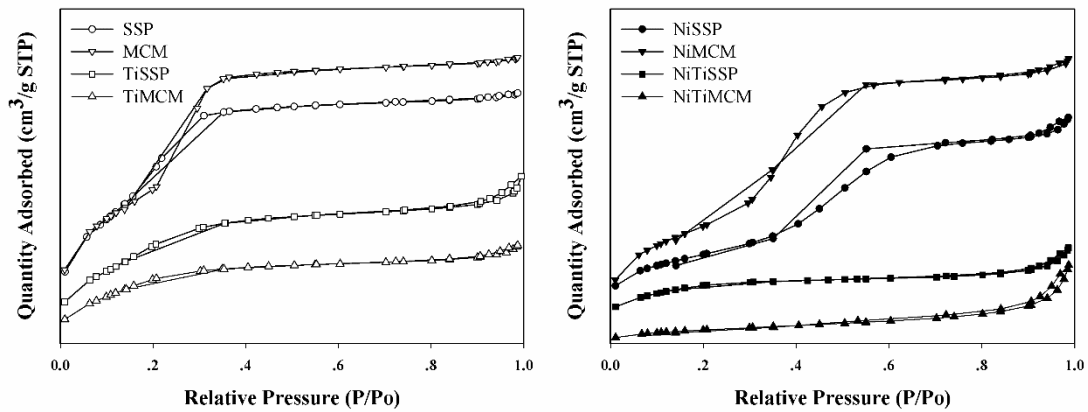


Fig. 3. N₂ adsorption-desorption isotherm of different supports (left) and different nickel catalysts (right).

Table 1. BET surface area, pore volume and pore diameter of supports and nickel catalysts.

Samples	S _A BET (m ² /g)	V _p (cm ³ /g)	D _{BJH} (nm)
SSP	927	0.81	2.04
MCM	1187	1.03	2.13
TiSSP	385	0.16	3.23
TiMCM	137	0.14	4.57
NiSSP	620	0.53	2.20
NiMCM	805	0.42	2.44
NiTiSSP	201	0.09	4.02
NiTiMCM	51	0.10	7.18

CO₂ hydrogenation (H₂/CO₂ = 10/1) under methanation condition was performed to determine the overall activity and product selectivity of all Ni catalysts. Hydrogenation of CO₂ was carried out at 220, 270 and 320°C under atmospheric pressure. The reaction results are summarized in Table 2.

Table 2. Activity and product selectivity of nickel catalysts.

Reaction temperature (°C)	Samples	Conversion (%) ^a		Rate ^c ($\frac{\times 10^2 \text{ gCH}_2}{\text{g}_{\text{cat}} \text{ h}}$)	Product selectivity ^c (%)	
		Initial ^b	Steady state ^c		CH ₄	CO
220	NiSSP	10	6	4.1	100.0	0.0
	NiMCM	18	16	11.5	100.0	0.0
	NiTiSSP	19	17	11.5	100.0	0.0
	NiTiMCM	22	19	12.8	100.0	0.0
270	NiSSP	45	37	25.8	99.0	1.0
	NiMCM	73	65	45.0	98.9	1.1
	NiTiSSP	77	74	50.3	100.0	0.0
	NiTiMCM	79	75	51.2	100.0	0.0
320	NiSSP	91	89	59.0	97.7	2.3
	NiMCM	96	90	60.4	97.5	2.5
	NiTiSSP	92	91	61.4	100.0	0.0
	NiTiMCM	96	95	65.0	100.0	0.0

^aCO₂ hydrogenation was carried out at 1 atm, and molar ratio of H₂/CO₂/Ar = 20/2/8, F/W = 18 L/g cat.h.

^b After 5 min of reaction.

^c After 6 h of reaction.

It can be observed that all Ni catalysts produced only methane upon the reaction temperature of 220°C (low temperature). The steady-state CO₂ conversions were ranged between 6 to 19% with corresponding to the reaction rate at 4.1 to 12.8 (x10² g CH₂/g cat.h). In addition, the steady-state CO₂ conversions distinctly increased when the reaction temperature was raised. For CO₂ hydrogenation, the operating temperature must be rather high [13]. The steady-state CO₂ conversions were ranged between 37 to 75% and 89 to 95% in accordance with the reaction temperature of 270 and 320°C, respectively. The obtained products consisting of methane and CO at high temperature confirmed that CO₂ hydrogenation over NiSSP and NiMCM catalysts occurred via a consecutive mechanism as shown in equations (1) and (2). First, CO₂ is converted to CO by the reverse water gas-shift (RWGS) reaction, and then CO is further hydrogenated to methane as follows;



However, the Ni catalysts supported on both TiSSP and TiMCM exhibited higher activity than those supported on SSP and MCM. Thus, the well dispersion of TiO₂ particles on SiO₂ surface increased the rate of CO hydrogenation reaction [14]. The oxygen uptake of TiO_x was also present due to oxygen can oxidize TiO_x to TiO₂. Furthermore, TiO_x promotes CO and CO₂ dissociation [15]. In addition, the selectivity to methane of NiTiSSP and NiTiMCM catalysts remain 100% during the high reaction temperatures (270 and 320°C). On the other word, with the presence of Ti in the composite oxide supports, the RWGS reaction was completely absent, especially at high reaction temperatures. Moreover, the lesser disparity of conversion between initial and steady-state indicated that the presence of Ti on supports also enhanced the stability of catalysts. TiO₂ could be mixed with some other oxides for improving surface characteristics, thermal stability and surface acidity of the composites catalysts and consequently their catalytic performances [1, 8]. The CO chemisorption was performed on the different Ni catalysts in order to determine the number of active sites as shown in Table 3. The amounts of CO adsorbed on the catalytic phase were ranged between 6 to 38 μmol CO/g of catalyst. The amount of reduced nickel metal active sites distinctly decreased with the addition of titania into the silica support. Surprisingly, the reaction rate of the nickel catalysts was not corresponding to the results obtained from CO chemisorption as seen from Table 3. On the other words, the results from catalytic testing and nickel dispersion are not consistent. For instance, the Ni supported on Ti-Si composite exhibited higher activity than that of Ni supported on silica based catalysts in spite of its lower Ni dispersion. This can be described that one possible reason for the lower CO chemisorption of NiTiSSP and NiTiMCM is likely because of the creation of the new Lewis acid sites during incorporation of titania and silica to form Ti-O-Si chemical bonds [16-18], which can act as electron acceptors to inhibit the CO chemisorption process [8]. As the result, the amounts of CO chemisorption of Ni on the Ti-Si composite supports were too low. Therefore, the more powerful technique, such as TEM was performed to determine the dispersion of Ni. There is also a good evidence to clarify that with TEM technique further.

Table 3. Maximum temperatures, reducibility from TPR profiles and Ni dispersion of nickel catalysts.

Catalysts	Maximum Temperature (°C)	Reducibility ^a (30-650°C) (%)	Total CO chemisorption (μmol CO/g.cat)	% dispersion of nickel ^b
NiSSP	380	42.9	38	1.12
NiMCM	365	35.0	35	1.03
NiTiSSP	384	43.0	6	0.17
NiTiMCM	391	38.2	23	0.68

^a Determined by TPR analysis

^b Determined by CO chemisorption

To elucidate the influence of element quantities on the catalytic activity, the catalyst samples were characterized by EDX and XPS analysis (Table 4). The EDX measures the elemental concentration in a layer less than 5 μm from the surface. The EDX data showed that the bulk nickel concentrations were ranged

between 23 and 26 wt%, while Ti contents were at 22.3 and 21.4 wt% for NiTiSSP and NiTiMCM, respectively. The XPS (The depth of XPS analysis is about 10Å) convinces the external surface element concentrations influencing on the catalytic activity. The XPS data indicated the remarkably high amount of Ni at the surface. Moreover, the amounts of Ni for all catalysts from XPS analysis were distinctly higher than EDX analysis. This indicated that the nickel oxides were mostly located on the external surface of catalysts. The distinctly large amounts at external surface of nickel concentration in NiTiSSP and NiTiMCM catalysts were in accordance with the higher catalytic activity than these of NiSSP and NiMCM catalysts. Furthermore, the complementary reason for the higher activity of NiTiMCM than that of NiTiSSP should be due to the Ti concentration at the external surface in NiTiMCM was larger than NiTiSSP as seen from the XPS data. The titania overlayer (TiO₂) may be important for the hydrogenation activity as mentioned before.

Table 4. XPS and EDX analysis of nickel catalysts.

Catalysts	Binding Energy (eV)			Surface element (%mass) ^a			Bulk element (%mass) ^b		
	Si 2p	Ti 2p	Ni 2p	Si	Ti	Ni	Si	Ti	Ni
NiSSP	94.70	-	855.80	44.67	-	55.33	75.56	-	24.44
	103.80		862.80						
NiMCM	94.70	-	855.50	47.33	-	52.66	76.69	-	23.31
	103.20		862.30						
NiTiSSP	102.60	459.65	855.30	8.90	17.61	73.48	51.62	22.28	26.10
		465.35	862.00						
NiTiMCM	102.80	459.15	855.10	15.40	19.57	65.04	53.33	21.40	25.27
		464.95	862.30						

^a Determined by XPS analysis

^b Determined by EDX analysis

In addition, XPS was also applied to obtain the information about the oxidation state and chemical environment of the elements present on the surface of the catalyst. The XPS data indicated that the two photoelectron peaks are nearly the same in the catalysts. The Ni 2p core level spectrum of NiO showed identical spectra (not shown) in the binding energy region of 855-856 eV and 872-874 eV for 2p_{3/2} and 2p_{1/2}, respectively [3, 7]. Previous research has reported the binding energy at 852.6, 854.6 and 856.1 eV for Ni 2p_{3/2} XPS spectra corresponding to Ni⁰, Ni²⁺ and Ni³⁺, respectively in oxidized Ni oxides, hydroxides and oxyhydroxides [19, 20]. However, there was no significant difference in the binding energy of Ni 2p with the addition of titania in the support. The position of binding energy for the Si 2p peaks were located at 94.7, 103.8 eV for NiSSP and 94.7, 103.2 eV for NiMCM. The binding energy at 94.7 eV was assigned to the occurrence of silicate (Si_xO_y except SiO₂) on the catalysts surface [8, 21]. The formation of surface silicates during preliminary steps of catalyst preparation was considered as a probably reason for partial reduction of the total nickel present at the temperatures normally used up to 500°C. However, the addition of titania onto the silica or silicon dioxide support of NiTiSSP and NiTiMCM apparently resulting in the absence of binding energy for surface silicate compound [27].

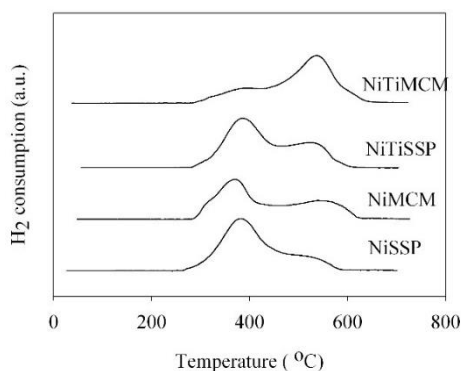


Fig. 4. TPR profiles of different nickel catalysts.

TPR measurements were executed to study the reduction behaviors of all nickel catalysts. The TPR profiles of Ni supported on different silica and Ti-Si composite supports are shown in Fig. 4. The nickel catalysts distinctly presented two overlap peaks of reduction located at ca. 300-600°C, one with a peak maximum at 390°C and another around 600°C. The low temperature peaks can be generally assigned to the reduction of the larger NiO particles, which are similar to the bulk NiO. This was in agreement with the peak at low temperature that in accordance with the reduction of large nickel oxide crystallite, having slight or no interaction with supports [22]. The high temperature peaks can be generally assigned to the reduction of the NiO strongly contacted with the oxide support [23]. Hence, the formation of smaller crystallite size of nickel oxide on the support resulting in strong metal-support interaction between nickel and oxide support [22]. This can be clearly observed that there is a significant variation in both low and high reduction temperatures. One possible reason for the NiSSP, NiMCM and NiTiSSP having reduction peaks located at the low reduction temperature was due to these catalysts generally were composed of mostly nickel oxides having large crystallite and slight or no interaction with oxide supports. However, the NiTiMCM catalyst exhibited the reduction behaviors that being quite different from other catalysts. The reduction peak of NiTiMCM is located at the high reduction temperature indicating most of nickel oxides of this sample were generally exhibited the strong interaction with oxide supports. The maximum temperature and reducibility results [24] for various nickel catalysts are summarized in Table 3. The maximum temperatures of NiSSP and NiMCM are located at ca. 380 and 365°C, respectively. After titania was introduced into the silica support, the maximum reduction temperatures were slightly shifted to higher temperature due to stronger interaction between nickel oxide species and the support. The metal-support interaction was corresponding to the temperature of both the low and high temperature reduction peaks that increases in sequence of Ni/SiO₂ < Ni/TiO₂ [25]. Moreover, the smaller nickel particle size exhibited the strong metal-support interaction leading to the higher reduction temperature. In addition, the reducibilities of NiTiSSP and NiTiMCM catalysts slightly increased with the addition of titania in the silica supports. The use of TiPOT for the preparation of Ti-Si composites apparently resulted in an increasing of the reducibility of cobalt [8] and nickel oxide [26]. Furthermore, previous reports suggested that the presence of Ti³⁺ in titania can enhance the reducibility [27]. One possible reason for the increased reducibility of NiTiSSP and NiTiMCM can be explained upon the absence of nickel silicate compound as mentioned earlier.

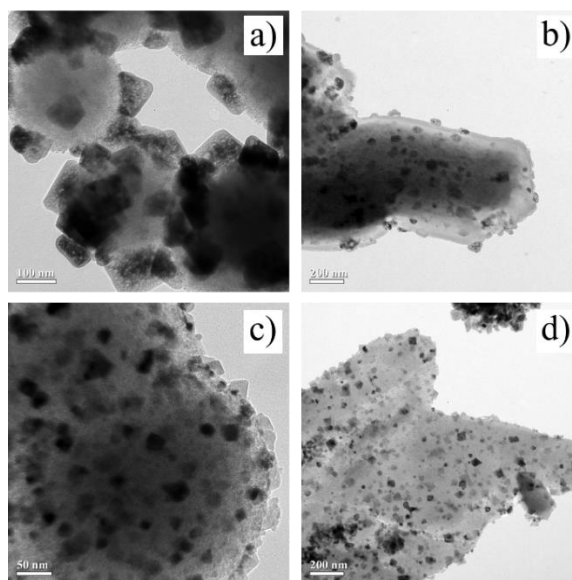


Fig. 5. TEM micrographs of nickel catalysts (a) NiSSP, (b) NiMCM, (c) NiTiSSP, and (d) NiTiMCM

The influences of titania addition on the metal dispersion of nickel catalysts were proven by TEM. Figure 5 shows the TEM micrographs of samples without titania addition (a, b) and with titania addition (c, d) catalysts. The dark patches represent the nickel oxides dispersing on the supports after calcination of catalysts. Figure 5 (a, b) shows that the nickel oxide species exhibit good distribution in the NiSSP and NiMCM. The nickel crystallites sizes were generally larger than 50 nm. After introduction of titania, Figs. 5

(c) and 5 (d) show that titania was well dispersed onto the surface of SSP and MCM. The transparent crystallites represent titania dispersing on the supports after calcination of catalysts. Moreover, Figs. 5 (c, d) displays the nickel oxide species having distinctly good distribution in the NiTiSSP and NiTiMCM. The TEM micrographs demonstrate that the titania crystallites on the SSP and MCM41 surface improve the dispersion of nickel oxide. This phenomenon was also observed with the titania in nickel oxide [1] and cobalt oxide [8] catalysts.

The comparative studies of hydrogenation to methane over various nickel catalysts are given in Table 5. It was observed that the NiTiMCM as developed in this study is very competitive among those typical and modified catalysts. Thus, the NiTiMCM can be promisingly applied for CO₂ hydrogenation.

Table 5. Summary of various catalysts for CO₂ hydrogenation to methane and their catalytic performance.

Catalyst	Amount of Catalyst (mg)	Space velocity (h ⁻¹)	Reaction temperature (°C)	Conversion (%)	CH ₄ selectivity (%)	Reference
Ni/TiMCM	100	GHSV 18,000	320	95	100	This work
Ni/SiO ₂ -RHA	50	GHSV 36,000	500	25-35	40-50	[4]
Ni/CeO ₂ -ZrO ₂	150	GHSV 20,000	275	55.0	99.8	[28]
Ni/TiO ₂	50	GHSV 60,000	350	73.2	99.8	[29]
Ni/Al ₂ O ₃	700	GHSV 15,000	500	74.0	83.8	[30]
Ni-Ce/CNT	100	GHSV 30,000	350	83.8	99.8	[31]
Ni/CaO-Al ₂ O ₃	50	GHSV 15,000	400	81.0	98.8	[32]
Ni/MgAl ₂ O ₃	200	GHSV 15,000	350	85.0	98-100	[33]
Ni/CeO ₂ -ZrO ₂	150	GHSV 43,000	350	67.9-79.7	98.4-99.3	[34]

4. Conclusion

In summary, the deposition of titania crystallites on the silica surface exhibits the robust characteristic and catalytic properties of nickel catalysts. First, it could prevent the nickel silicates formation as measured by XPS and TPR. Secondly, the titania crystallites provide the improvement of nickel oxide distribution in the support granules that was observed by TEM analysis. Finally, it promotes CO and CO₂ dissociation resulting in complete inhibition of RWGS reaction (absence of CO product), especially at high reaction temperature. Therefore, the nickel catalysts supported on Ti-Si composite oxides show good stability in catalytic hydrogenation, where the initial and steady state conversion slightly decreased with the presence of titania on the silica surface.

Acknowledgement

The authors thank the Thailand Research Fund (IRG5780014) and Grant for International Research Integration: Chula Research Scholar, Ratchadaphiseksompot Endowment Fund for financial support of this project. We also would like to thank the Postdoctoral Scholarship (Chulalongkorn University) for supporting this research.

References

- [1] J. R. Grzechowiak, I. Szyszka, J. Rynkowski, and D. Rajski, "Preparation, characterisation and activity of nickel supported on silica-titania," *Appl. Catal., A: Gen.*, vol. 247, pp. 193-206, 2003.
- [2] W. Pan and C. Song, "Using tapered element oscillating microbalance for in situ monitoring of carbon deposition on nickel catalyst during CO₂ reforming of methane," *Catal. Today*, vol. 148, pp. 232-242, 2009.
- [3] E. Heracleous, A. F. Lee, K. Wilson, and A. A. Lemonidou, "Investigation of Ni-based alumina-supported catalysts for the oxidative dehydrogenation of ethane to ethylene: structural characterization and reactivity studies," *J. Catal.*, vol. 231, pp. 159-171, 2005.
- [4] F.-W. Chang, M.-T. Tsay, and S.-P. Liang, "Hydrogenation of CO₂ over nickel catalysts supported on rice husk ash prepared by ion exchange," *Appl. Catal., A: Gen.*, vol. 209, pp. 217-227, 2001.

- [5] A. E. Aksoylu and Z. İlsenÖnsan, “Hydrogenation of carbon oxides using coprecipitated and impregnated Ni/Al₂O₃ catalysts,” *Appl. Catal., A: Gen.*, vol. 164, pp. 1-11, 1997.
- [6] G. D. Weatherbee and C. H. Bartholomew, “Hydrogenation of CO₂ on group VIII metals: II. Kinetics and mechanism of CO₂ hydrogenation on nickel,” *J. Catal.*, vol. 77, pp. 460-472, 1982.
- [7] C. Cheng, D. Shen, R. Xiao, and C. Wu, “Methanation of syngas (H₂/CO) over the different Ni-based catalysts,” *Fuel*, vol. 189, pp. 419-427, 2017.
- [8] J. Janlamool, P. Praserthdam, and B. Jongsomjit, “Ti-Si composite oxide-supported cobalt catalysts for CO₂ hydrogenation,” *J. Nat. Gas Chem.*, vol. 20, pp. 558-564, 2011.
- [9] K. Pinkaew, O. Mekasuwandumrong, J. Panpranot, A. Shotipruk, P. Praserthdam, J. G. Goodwin Jr., and B. Jongsomjit, “Zirconia modification on nanocrystalline titania-supported cobalt catalysts for methanation,” *Engineering Journal*, vol. 16, no. 4, pp. 29-37, 2012.
- [10] S. Medsforth, “CLXIX.-Promotion of catalytic reactions. Part I,” *J. chem. Soc. Trans.*, vol. 123, pp. 1452-1469, 1923.
- [11] Z.-H. Suo, Y. Kou, J.-Z. Niu, W.-Z. Zhang, and H.-L. Wang, “Characterization of TiO₂-, ZrO₂- and Al₂O₃-supported iron catalysts as used for CO₂ hydrogenation,” *Appl. Catal., A: Gen.*, vol. 148, pp. 301-313, 1997.
- [12] J. Kruatim, S. Jantasee, and B. Jongsomjit, “Improvement of cobalt dispersion on Co/SBA-15 and Co/SBA-16 catalysts by ultrasound and vacuum treatments during post-impregnation step,” *Engineering Journal*, vol. 21, no. 1, pp. 17-28, 2017.
- [13] T. Riedel, M. Claeys, H. Schulz, G. Schaub, S.-S. Nam, K.-W. Jun, M.-J. Choi, G. Kishan, and K.-W. Lee, “Comparative study of Fischer–Tropsch synthesis with H₂/CO and H₂/CO₂ syngas using Fe- and Co-based catalysts,” *Appl. Catal., A: Gen.*, vol. 186, pp. 201-213, 1999.
- [14] E. I. Ko and F. H. Rogan, “Metal-support interactions for nickel supported on a titania-silica surface phase oxide,” *Chem. Eng. Commun.*, vol. 55, pp. 139-148, 1987.
- [15] J. van de Loosdrecht, A. M. van der Kraan, A. J. van Dillen, and J. W. Geus, “Metal-support interaction: Titania-supported and silica-supported nickel catalysts,” *J. Catal.*, vol. 170, pp. 217-226, 1997.
- [16] S. Liu, P. Cool, O. Collart, P. Van Der Voort, E. F. Vansant, O. I. Lebedev, G. Van Tendeloo, and M. Jiang, “The influence of the alcohol concentration on the structural ordering of mesoporous silica: Cosurfactant versus cosolvent,” *J. Phys. Chem. B*, vol. 107, pp. 10405-10411, 2003.
- [17] R. Jin, Z. Wu, Y. Liu, B. Jiang, and H. Wang, “Photocatalytic reduction of NO with NH₃ using Si-doped TiO₂ prepared by hydrothermal method,” *J. Hazard. Mater.*, vol. 161, pp. 42-48, 2009.
- [18] J. Lu, K. M. Kosuda, R. P. Van Duyne, and P. C. Stair, “Surface acidity and properties of TiO₂/SiO₂ catalysts prepared by atomic layer deposition: UV–visible diffuse reflectance, DRIFTS, and visible Raman spectroscopy studies,” *J. Phys. Chem. C*, vol. 113, pp. 12412-12418, 2009.
- [19] M. W. Roberts and R. S. C. Smart, “The defect structure of nickel oxide surfaces as revealed by photoelectron spectroscopy,” *J. Chem. Soc., Faraday Trans. 1 F*, vol. 80, pp. 2957-2968, 1984.
- [20] A. F. Carley, S. D. Jackson, J. N. O’Shea, and M. W. Roberts, “The formation and characterisation of Ni³⁺—An X-ray photoelectron spectroscopic investigation of potassium-doped Ni(110),” *Surf. Sci.*, vol. 440, pp. L868-L874, 1999.
- [21] K. Arnby, M. Rahmani, M. Sanati, N. Cruise, A. A. Carlsson, and M. Skoglundh, “Characterization of Pt/γ-Al₂O₃ catalysts deactivated by hexamethyldisiloxane,” *Appl. Catal., B*, vol. 54, pp. 1-7, 2004.
- [22] F.-W. Chang, T.-J. Hsiao, S.-W. Chung, and J.-J. Lo, “Nickel supported on rice husk ash—Activity and selectivity in CO₂ methanation,” *Appl. Catal., A: Gen.*, vol. 164, pp. 225-236, 1997.
- [23] G. Gonçalves, M. K. Lenzi, O. A. A. Santos, and L. M. M. Jorge, “Preparation and characterization of nickel based catalysts on silica, alumina and titania obtained by sol–gel method,” *J. Non-Cryst. Solids*, vol. 352, pp. 3697-3704, 2006.
- [24] Y. Zhang, D. Wei, S. Hammache, and J. G. Goodwin, “Effect of water vapor on the reduction of Ru-promoted Co/Al₂O₃,” *J. Catal.*, vol. 188, pp. 281-290, 1999.
- [25] A. M. Diskin, R. H. Cunningham, and R. M. Ormerod, “The oxidative chemistry of methane over supported nickel catalysts,” *Catal. Today*, vol. 46, pp. 147-154, 1998.
- [26] J. R. Grzechowiak, I. Szyszka, and A. Masalska, “Effect of TiO₂ content and method of titania–silica preparation on the nature of oxidic nickel phases and their activity in aromatic hydrogenation,” *Catal. Today*, vol. 137, pp. 433-438, 2008.
- [27] K. Suriye, P. Praserthdam, and B. Jongsomjit, “Impact of Ti³⁺ present in titania on characteristics and catalytic properties of the Co/TiO₂ Catalyst,” *Ind. Eng. Chem. Res.*, vol. 44, pp. 6599-6604, 2005.

- [28] J. Ashok, M. L. Ang, and S. Kawi, "Enhanced activity of CO₂ methanation over Ni/CeO₂-ZrO₂ catalysts: Influence of preparation methods," *Catal. Today*, vol. 281, Part 2, pp. 304-311, 2017.
- [29] R. Zhou, N. Rui, Z. Fan, and C.-J. Liu, "Effect of the structure of Ni/TiO₂ catalyst on CO₂ methanation," *Int. J. Hydrogen Energy*, vol. 41, pp. 22017-22025, 2016.
- [30] G. Garbarino, D. Bellotti, P. Riani, L. Magistri, and G. Busca, "Methanation of carbon dioxide on Ru/Al₂O₃ and Ni/Al₂O₃ catalysts at atmospheric pressure: Catalysts activation, behaviour and stability," *Int. J. Hydrogen Energy*, vol. 40, pp. 9171-9182, 2015.
- [31] W. Wang, W. Chu, N. Wang, W. Yang, and C. Jiang, "Mesoporous nickel catalyst supported on multi-walled carbon nanotubes for carbon dioxide methanation," *Int. J. Hydrogen Energy*, vol. 41, pp. 967-975, 2016.
- [32] B. Mutz, H. W. P. Carvalho, S. Mangold, W. Kleist, and J.-D. Grunwaldt, "Methanation of CO₂: Structural response of a Ni-based catalyst under fluctuating reaction conditions unraveled by operando spectroscopy," *J. Catal.*, vol. 327, pp. 48-53, 2015.
- [33] Z. Fan, K. Sun, N. Rui, B. Zhao, and C.-J. Liu, "Improved activity of Ni/MgAl₂O₄ for CO₂ methanation by the plasma decomposition," *J. Energy Chem.*, vol. 24, pp. 655-659, 2015.
- [34] P. A. U. Aldana, F. Ocampo, K. Kobl, B. Louis, F. Thibault-Starzyk, M. Daturi, P. Bazin, S. Thomas, and A.C. Roger, "Catalytic CO₂ valorization into CH₄ on Ni-based ceria-zirconia. Reaction mechanism by operando IR spectroscopy," *Catal. Today*, vol. 215, pp. 201-207, 2013.